Neuropsychopharmacology (2017) 42, 649–660

www.neuropsychopharmacology.org

Pharmacokinetic Profiles and Pharmacodynamic Effects for Methylone and Its Metabolites in Rats

Joshua S Elmore[1], Ora Dillon-Carter[1], John S Partilla[1], Kayla N Ellefsen[2,3], Marta Concheiro[2,4], Masaki Suzuki[5], Kenner C Rice[5], Marilyn A Huestis[2] and Michael H Baumann*[,1]

[1]Designer Drug Research Unit, Intramural Research Program, National Institute on Drug Abuse, National Institutes of Health, Baltimore, MD, USA; [2]Chemistry & Drug Metabolism Section, Intramural Research Program, National Institute on Drug Abuse, National Institutes of Health, Baltimore, MD, USA; [3]Program in Toxicology, University of Maryland at Baltimore, Baltimore, MD, USA; [4]Department of Sciences, John Jay College of Criminal Justice, City University of New York, New York, NY, USA; [5]Drug Design and Synthesis Section, Intramural Research Program, National Institute on Drug Abuse, National Institutes of Health, Baltimore, Maryland, USA

3,4-Methylenedioxy-*N*-methylcathinone (methylone) is a new psychoactive substance and the β-keto analog of 3,4-methylenedioxy-*N*-methylamphetamine (MDMA). It is well established that MDMA metabolism produces bioactive metabolites. Here we tested the hypothesis that methylone metabolism in rats can form bioactive metabolites. First, we examined the pharmacokinetics (PKs) of methylone and its metabolites after subcutaneous (sc) methylone administration (3, 6, 12 mg/kg) to male rats fitted with intravenous (iv) catheters for repeated blood sampling. Plasma specimens were assayed by liquid chromatography tandem mass spectrometry to quantify methylone and its phase I metabolites: 3,4-methylenedioxycathinone (MDC), 3,4-dihydroxy-*N*-methylcathinone (HHMC), and 4-hydroxy-3-methoxy-*N*-methylcathinone (HMMC). The biological activity of methylone and its metabolites was then compared using *in vitro* transporter assays and *in vivo* microdialysis in rat nucleus accumbens. For the PK study, we found that methylone and MDC peaked early (T_{max} = 15-45 min) and were short lived ($t_{1/2}$ = 60–90 min), while HHMC and HMMC peaked later (T_{max} = 60-120 min) and persisted ($t_{1/2}$ = 120–180 min). Area-under-the-curve values for methylone and MDC were greater than dose-proportional, suggesting non-linear accumulation. Methylone produced significant locomotor activation, which was correlated with plasma methylone, MDC, and HHMC concentrations. Methylone, MDC, and HHMC were substrate-type releasers at monoamine transporters as determined *in vitro*, but only methylone and MDC (1, 3 mg/kg, iv) produced significant elevations in brain extracellular dopamine and 5-HT *in vivo*. Our findings demonstrate that methylone is extensively metabolized in rats, but MDC is the only centrally active metabolite that could contribute to overall effects of the drug *in vivo*. *Neuropsychopharmacology* (2017) **42,** 649–660; doi:10.1038/npp.2016.213; published online 26 October 2016

INTRODUCTION

Synthetic cathinones are a class of new psychoactive substances with structural and pharmacological similarity to amphetamines (Glennon, 2014). Various cathinone analogs appeared in the United States recreational drug market during 2010 and 2011 and were sold under false pretenses as 'bath salts', 'plant food' or 'research chemicals' to circumvent legislative and regulatory efforts (Baumann *et al*, 2013). The cathinones most commonly found in early bath salts included 3,4-methylenedioxypyrovalerone, (±)-3,4-methylenedioxy-*N*-methylcathinone HCl (methylone) and 4-methyl-*N*-methylcathinone. These substances were placed into emergency schedule I control in 2011 by the US Drug Enforcement Administration (DEA), and were later permanently scheduled (Drug Enforcement Administration DoJ, 2011, 2013). Despite these legislative efforts, reports by the DEA revealed that the prevalence of methylone increased from 2011 to 2013, and as of 2014, methylone was encountered as often as the club drug 3,4-methylenedioxy-*N*-methylamphetamine (MDMA) (NFLIS Special Report, 2014; NFLIS 2014 Annual Report). Recreational users take methylone for its euphoric and stimulant properties, but it can cause life-threatening adverse effects, including hyperthermia, seizures, and kidney damage; its use has led to several analytically confirmed fatalities (Barrios *et al*, 2015; Carbone *et al*, 2013; Cawrse *et al*, 2012; Kovacs *et al*, 2012; Ridpath *et al*, 2014; Warrick *et al*, 2012).

From a pharmacological perspective, methylone exerts its effects by acting as a substrate at the plasma membrane transporters for dopamine (DAT), norepinephrine (NET), and 5-HT (SERT), thereby inducing non-exocytotic release of these monoamine transmitters (Baumann *et al*, 2012; Eshleman *et al*, 2013; Simmler *et al*, 2013). *In vivo* studies in rats demonstrate that methylone increases extracellular

*Correspondence: Dr MH Baumann, Designer Drug Research Unit, Intramural Research Program, National Institute on Drug Abuse, National Institutes of Health, 333 Cassell Drive, Suite 4400, Baltimore, MD 21224, USA, Tel: +1 443 740-2660, Fax: +1 443 740 2241, E-mail: mbaumann@mail.nih.gov
Received 19 April 2016; revised 5 September 2016; accepted 10 September 2016; accepted article preview online 23 September 2016

concentrations of dopamine and 5-HT in the brain, with greater effects on 5-HT (Baumann *et al*, 2012; Schindler *et al*, 2016). The mechanism of action for methylone resembles that of MDMA, which is not surprising considering methylone is the β-keto analog of MDMA. It is notable that MDMA is metabolized by hepatic mechanisms in rats and humans (de la Torre and Farre, 2004), and its bioactive metabolites may contribute to the profile of drug effects *in vivo* (Concheiro *et al*, 2014; Schindler *et al*, 2014). Moreover, MDMA displays non-linear pharmacokinetics (PKs) characterized by increases in plasma drug concentrations that are greater than dose-proportional (Baumann *et al*, 2009; Chu *et al*, 1996; de la Torre *et al*, 2000).

Few studies have examined methylone metabolism and PKs *in vivo*. Kamata *et al* (2006) first evaluated methylone metabolism by determining parent and metabolite concentrations in urine from rats and humans exposed to methylone. These investigators showed that methylone is metabolized in a manner akin to MDMA involving two major pathways (Figure 1): (1) *O*-demethylenation to form (±)-3,4-dihydroxy-*N*-methylcathinone (HHMC) followed by *O*-methylation to form (±)-4-hydroxy-3-methoxy-*N*-methylcathinone (HMMC) and (2) *N*-demethylation to produce (±)-3,4-methylenedioxycathinone (MDC) (Kamata *et al*, 2006). Methylone is primarily biotransformed by cytochrome p450 2D6 (CYP2D6) in humans, the same isoform responsible for metabolism of MDMA (Pedersen *et al*, 2013). Lopez-Arnau *et al* (2013) evaluated methylone PK and pharmacodynamic effects in rats and found that methylone exhibits rapid kinetics, with peak blood concentrations occurring 30 min after oral administration, and readily crosses the blood–brain barrier (Lopez-Arnau *et al*, 2013). In the study of Lopez-Arnau *et al* (2013), methylone concentrations in plasma correlated with locomotor activation, although the authors speculated that metabolites may also be bioactive. Importantly, the plasma PK profiles for the metabolites of methylone have not been reported, and the potential bioactivity of methylone metabolites has yet to be systematically evaluated.

Ellefsen *et al* (2015) reported a highly sensitive validated assay for the quantification of methylone, MDC, HHMC, and HMMC using liquid chromatography tandem mass spectrometry (LC–MS/MS) (Ellefsen *et al*, 2015). In the present study, we utilized this new analytical method to test the hypothesis that methylone is metabolized in rats to form bioactive metabolites. In particular, we examined plasma concentrations of methylone and its metabolites after systemic administration of methylone at multiple doses (3, 6, and 12 mg/kg). We employed the subcutaneous (sc) route of administration for the PK studies to allow for the comparison of our data with the results of others who examined pharmacological effects of sc methylone in rats (Baumann *et al*, 2012; Grecco and Sprague, 2016; Kiyatkin *et al*, 2015; Lopez-Arnau *et al*, 2014). Our experiments employed freely moving rats fitted with indwelling jugular catheters, which enabled repeated assessment of PK and pharmacodynamic end points in the same individuals. Next we examined the neurobiological effects of methylone and its metabolites using *in vitro* transporter release assays and *in vivo* microdialysis in the rat brain. Overall, our findings demonstrate that methylone is extensively metabolized after systemic administration and displays non-linear accumulation in plasma. In addition, MDC and HHMC are potent substrates at monoamine transporters *in vitro*, but only MDC induces centrally mediated neurochemical effects *in vivo*.

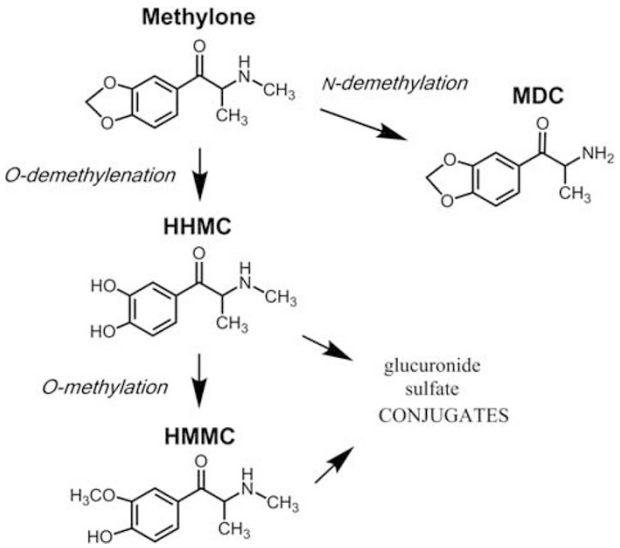

Figure 1 Pathways of methylone metabolism. Methylone, 3,4-methylenedioxy-*N*-methylcathinone; MDC, 3,4-methylenedioxycathinone; HHMC, 3,4-dihydroxy-*N*-methylcathinone; HMMC, 4-hydroxy-3-methoxy-*N*-methylcathinone.

MATERIALS AND METHODS

Drugs and Reagents

(±)-3,4-Methylenedioxy-*N*-methylcathinone HCl (methylone) was obtained from the National Institute on Drug Abuse (NIDA) Drug Supply Program (Rockville, MD, USA). MDC HCl, HHMC HBr, and HMMC HCl were synthesized as previously described (Ellefsen *et al*, 2015). [^{3}H]1-methyl-4-phenylpyridinium ([^{3}H]MPP+, specific activity = 85 Ci/mmol) was purchased from American Radiolabeled Chemicals (St Louis, MO, USA), whereas [^{3}H]serotonin ([^{3}H]5-HT, specific activity = 20 Ci/mmol) was purchased from Perkin Elmer (Shelton, CT, USA). All other chemicals and reagents required for LC–MS/MS, *in vitro* transporter assays, *in vivo* microdialysis methods, and high-performance liquid chromatography with electrochemical detection (HPLC-ECD) were obtained from Sigma-Aldrich (St Louis, MO, USA) unless otherwise noted.

Animals and Surgery

Male Sprague-Dawley rats weighing 250–300 g were group-housed (lights on: 0700–1900 hours) under controlled temperature (22 ± 2 °C) and humidity (45% ± 5%) with free access to food and water. Experiments were performed in accordance with the National Institutes of Health Guide for the Care and Use of Laboratory Animals. Vivarium facilities were fully accredited by the Association for Assessment and Accreditation of Laboratory Animal Care, and study procedures were approved by the NIDA IRP Animal Care and Use Committee. After 2 weeks of acclimation to the

vivarium, rats were used for tissue harvest or subjected to surgical procedures and subsequently used for experiments. A total of 75 rats were used for these studies: 25 for the PK experiments, 16 for the *in vitro* transporter assays, and 34 for the *in vivo* microdialysis experiments.

For the PK experiments, rats were anesthetized with 60 mg/kg intraperitoneal (ip) sodium pentobarbital. Each rat received a surgically implanted IPTT-300 transponder (Bio Medic Data Systems, Seaford, DE, USA) to facilitate non-invasive measurement of body temperature via a handheld radio frequency reader system. Transponders were $14 \times 2\,mm^2$ cylinders and were implanted sc posterior to the shoulder blades via a sterile guide needle. Immediately after transponder implantation, each rat received a surgically implanted catheter in the right jugular vein (Baumann *et al*, 2012). In brief, the proximal Silastic end of the catheter was inserted into the right jugular vein and advanced to the atrium, whereas the distal vinyl end was exteriorized on the nape and plugged with a metal stylet. Animals were individually housed postoperatively and allowed 7–10 days for recovery.

For the *in vivo* microdialysis experiments, rats were anesthetized with 60 mg/kg ip sodium pentobarbital. Each rat received a surgically implanted jugular catheter as described above. Immediately after the catheter surgery, rats were placed into a stereotaxic apparatus and a CMA12 intracerebral guide cannula (Harvard Apparatus, Holliston, MA, USA) was implanted above the nucleus accumbens, according to the stereotaxic coordinates: 1.6 mm lateral and 1.6 mm anterior to bregma, and 6.0 mm below the surface of the dura. Guide cannulae were secured to the skull using stainless steel anchor screws and dental acrylic. Animals were individually housed postoperatively and allowed 7–10 days for recovery.

PK Experiments

Rats were moved to the testing room in their home cages and given 1 h to acclimate. Feeding trays were removed, and wire lids were placed atop the cages. Polyethylene extension tubes (30 cm) were filled with sterile saline, connected to iv catheters, and threaded outside the cages. Catheters were flushed with 0.3 ml of 48 IU/ml heparin saline to facilitate blood withdrawal. Groups of rats received sc injections of 0 (saline), 3, 6, or 12 mg/kg methylone in a volume of 1 ml/kg. Blood specimens (0.30 ml) were withdrawn immediately before injection and at 15 min, 30 min, 1, 2, 4, and 8 h thereafter. Blood was collected into 1 ml syringes, transferred to 1.5 ml plastic tubes fortified with 5 µl of sodium metabisulfite (250 nM) and 5 µl heparin (1000 IU), and centrifuged for 10 min at 3000 rpm; plasma was decanted and stored at − 80 °C. An equal volume of sterile saline was infused after each blood withdrawal to maintain volume and osmotic homeostasis.

Behavior was monitored for a period of 1 min before blood sampling, and each rat was assigned a locomotor activity score based upon the following parameters: 1 = asleep or still; 2 = in-place activities; 3 = locomotion, rearing, or sniffing; 4 = any two (locomotion, rearing, or sniffing); 5 = 10 s of continuous sniffing without locomotion or rearing; 6 = 10 s of continuous sniffing with locomotion or rearing; 7 = 5 s of patterned sniffing; 8 = 10 s of patterned sniffing. Patterned sniffing was defined as any repeated head motion (eg, up and down 'head bobbing') that occurred simultaneously with sniffing behavior. After observation, core temperatures were measured via a handheld radio frequency scanner, which acquired data via the implanted transponder.

Quantification of Methylone and Metabolites in Plasma

Plasma specimens were analyzed using LC–MS/MS, as previously described (Ellefsen *et al*, 2015). Briefly, 10 µl of β-glucuronidase was added to 100 µl of plasma to hydrolyze metabolite conjugates. Specimens were incubated at 50 °C for 60 min. Twenty microliters of 1 mg/ml 4-methylcatechol and 10 µl of concentrated perchloric acid were added, and the tubes were centrifuged at 15 000 *g* for 10 min. Supernatants were then loaded onto preconditioned cation exchange solid-phase-extraction cartridges and washed with 1 M acetic acid (500 µl) and methanol (500 µl) before eluting with 5% ammonium hydroxide in methylene chloride/isopropanol (60 : 40 v/v). Extracts were evaporated to dryness under nitrogen for 20 min at 40 °C after adding 50 µl of acidic methanol (1% HCl) to prevent analyte loss, before reconstitution in 200 µl of mobile phase A (0.1% formic acid in water).

Specimens were transferred into autosampler vials and LC–MS/MS analysis was performed on a Shimadzu liquid chromatography (LC) system (Columbia, MD, USA) coupled with an ABSciex 3200 QTrap mass spectrometer with a TurboIon Spray source (Foster City, CA, USA). Chromatographic separation was performed with a Synergi Polar-RP 100 A, $100 \times 2\,mm^2$, 4 µm column (Phenomenex, Torrance, CA, USA) with gradient elution performed with 0.1% formic acid in water (mobile phase A) and 0.1% formic acid in acetonitrile (mobile phase B). Mass spectrometric data were acquired in positive electrospray ionization mode with the following source parameters: IonSpray voltage 3500 V; temperature 600 °C; curtain gas 50; ion source gas 150 and ion source gas 230. Analytes were determined by two multiple reaction monitoring transitions. During method development, it was noted that HHMC exhibited high bias and imprecision, thus HHMC concentrations reported here are considered semiquantitative.

In Vitro Transporter Release Assays

Rats were killed by CO_2 narcosis, and the brains were processed to yield synaptosomes (Rothman *et al*, 2001). One whole brain minus caudate and cerebellum (for SERT and NET assays) or one pair of caudates (for DAT assays) was diluted in 10 ml of ice-cold 10% sucrose containing 1 µM reserpine. Tissue was homogenized using a Potter-Elvehjem homogenizer, centrifuged at 1000 *g* for 10 min at 4 °C, and supernatants (ie, synaptosomal preparations) were retained on ice. Supernatants were diluted with sucrose solution to yield protein concentrations of 900 µg/ml for SERT and NET assays and 90 µg/ml for DAT assays. *In vitro* release assays were conducted using $[^3H]MPP^+$ as the radiolabeled substrate for DAT and NET, while using $[^3H]$5-HT as the radiolabeled substrate for SERT.

Synaptosomes were incubated to steady state in a polypropylene beaker, with stirring at 25 °C, in Krebs phosphate buffer (pH 7.4), which contained 1 µM reserpine

and either 5 nM [^{3}H]MPP$^+$ or 5 nM [^{3}H]5-HT. To commence the assay, 850 µl of preloaded synaptosomes were added to polystyrene test tubes or 96-well plates that contained 150 µl test drug in uptake buffer plus 1 mg/ml bovine serum albumin. Eight-point dilution curves, with doses ranging from 10 to 10 000 nM, were performed in triplicate on three separate occasions for each test drug. After 30 min ([^{3}H]MPP$^+$assays) or 5 min ([^{3}H]5-HT assays), the release reaction was terminated by dilution with 4 ml wash buffer (10 mM Tris-HCl pH 7.4 containing 0.9% NaCl at 25 °C) followed by rapid vacuum filtration over Whatman GF/B filters using a Brandel cell harvester (Brandel, Gaithersburg, MD, USA). Filters were rinsed twice with 4 ml wash buffer and dried under vacuum. The retained tritium was counted by a liquid scintillation counter at 40% efficiency after an overnight extraction in 0.6 ml scintillation cocktail. It is important to note that the amount of tritium retained is inversely proportional to the extent of release from synaptosomes; that is, a lower amount of retained tritium reflects a higher degree of transporter-mediated release. Drug potency is expressed as the molar concentration required to evoke 50% of maximal release (EC_{50}), where maximal release is defined in the presence of saturating concentrations of the non-specific transporter substrate, tyramine: 10 µM tyramine for DAT and NET assays or 100 µM tyramine for SERT assays.

In Vivo Microdialysis Procedures

In vivo microdialysis sampling was carried out as previously described, with minor modifications (Baumann *et al*, 2012). On the evening before an experiment, rats were moved to the testing room. A plastic collar was placed around the neck of each rat, a dialysis probe (CMA/12, Harvard Apparatus) was inserted into the guide cannula, and an extension tube was attached to the indwelling jugular catheter. The probe exchange surface was 2 × 0.5 mm. Each rat was placed into its own activity field arena and connected to a tethering system, which allowed motor activity within the container. Probes were perfused overnight with artificial cerebrospinal fluid pumped at a flow rate of 0.6 µl/min. On the next morning, dialysate samples were collected at 20 min intervals. Samples were immediately assayed for dopamine and 5-HT by HPLC-ECD. Chromatographic data were acquired online and exported to an Empower software system (Waters Associates, Milford, MA, USA) for peak amplification, integration, and analysis.

Rats were randomly assigned to groups receiving either drug (methylone, MDC, HHMC, or HMMC) or saline injections. Once three stable baseline samples were obtained, rats received two sequential iv injections of drug, 1 mg/kg at time 0, followed by 3 mg/kg 60 min later. Control rats received sequential iv injections of saline (1 ml/kg) according to the same schedule. We employed the iv route of administration for the microdialysis studies because this route affords a rapid assessment of drug effects while minimizing drug metabolism. Furthermore, the iv doses determined in the present study can be used as a guide for subsequent iv self-administration experiments if warranted. Microdialysis samples were collected every 20 min throughout the postinjection period for 120 min. At the end of the experiment, rats were killed with CO_2 and decapitated. Brain sections were examined to verify placement of microdialysis probe tips within the nucleus accumbens. Only those rats with correct placements were included in data analyses. During the overnight acclimation period and while undergoing microdialysis, each rat was housed within a square Plexiglass arena (43 length × 43 width × 43 height (cm^3)) equipped with a TruScan activity monitoring system (Coulbourn Instruments, Holliston, MA, USA), which was used to quantify horizontal locomotor activity. Horizontal locomotor activity was defined as the total distance traveled in the horizontal plane (measured in cm).

Data Analysis and Statistics

Data from PK experiments, *in vitro* release assays, and *in vivo* microdialysis were tabulated, analyzed, and graphically depicted using GraphPad Prism (version 5.04; GraphPad Software, La Jolla, CA). Plasma PK data were further analyzed using WinNonlin (version 6.3; Pharsight, Mountain View, CA) to determine non-compartmental PK constants. To evaluate possible non-linearity for plasma analyte concentrations, area-under-the-curve (AUC) values following 3 mg/kg were multiplied by 2 and 4 to calculate expected AUCs for 6 and 12 mg/kg doses, respectively. The expected values from the 6 and 12 mg/kg doses were compared with observed results by two-way ANOVA (treatment × condition), followed by Bonferroni's *post hoc* tests. Dose–response data from *in vitro* release experiments were subjected to nonlinear regression and expressed as the percentage of maximal release. Potency estimates are given as EC_{50} values determined from the fitted curves. Behavioral data were analyzed using a non-parametric Friedman's test followed by Dunn's multiple comparison test, whereas temperature data were evaluated by two-way analysis of variance (treatment × time), followed by Bonferroni's *post hoc* test. Neurochemical and locomotor data from the microdialysis experiments were analyzed by two-way analysis of variance (treatment × time) followed by Bonferroni's *post hoc* test. $p < 0.05$ was considered the minimal criterion for statistical significance.

RESULTS

PKs of Methylone and its Metabolites

Figure 2 depicts time–concentration profiles for plasma methylone, MDC, HHMC, and HMMC after sc injection of 3, 6, and 12 mg/kg methylone. The PK constants derived from the data depicted in Figure 2 are presented in Table 1. Methylone plasma concentrations increased in a dose-related manner. C_{max} values for methylone were 620, 1410, and 3170 µg/l for the 3, 6, and 12 mg/kg doses, while corresponding AUC values were 26 800, 68 300 and 201 000 min × µg/l. Methylone exhibited rapid kinetics with a T_{max} value of 15 min after all doses and $t_{1/2}$ values of 48, 57, and 66 min for 3, 6, and 12 mg/kg, respectively. MDC C_{max} values were about 10-fold lower than those for methylone across all doses, while MDC AUC values were roughly three times lower when compared with methylone. MDC exhibited slower kinetics than methylone, with T_{max} values of 30, 35, and 45 min and $t_{1/2}$ values of 64, 70, and 88 min for 3, 6, and 12 mg/kg methylone.

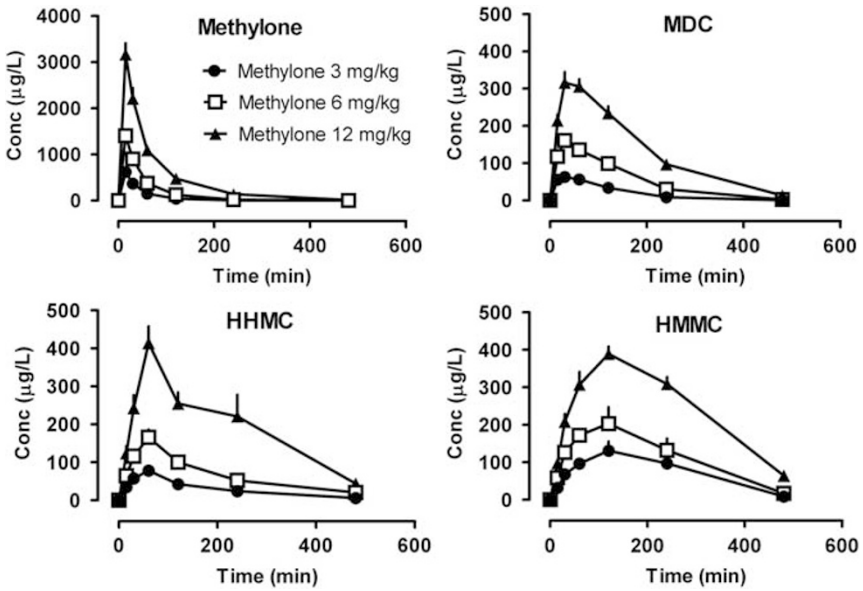

Figure 2 Concentration–time profiles for methylone, MDC, HHMC, and HMMC after sc administration of methylone. Data are mean ± SEM for $N = 6/7$ rats per group. Rats received a sc dose of 0 (saline), 3, 6, or 12 mg/kg methylone, and blood was collected at 15, 30, 60, 120, 240, and 480 min postinjection. Plasma was separated and analyzed by LC–MS/MS.

Table 1 Pharmacokinetic Constants (Mean ± SEM) for Plasma Methylone, MDC, HHMC, and HMMC After sc Methylone Injection at 3, 6, or 12 mg/kg to Rats ($N = 6$–7 per Group)

Analytes	Dose (mg/kg)	C_{max}(µg/l)	T_{max} (min)	AUC (min × µg/l)	$t_{½}$(min)	C_{last}(µg/l)
Methylone	3	620 ± 83	15	26 800 ± 3600	48 ± 12	3.5 ± 2.4
	6	1410 ± 95	15	68 300 ± 6500	57 ± 3	1.6 ± 0.7
	12	3170 ± 590	15	201 000 ± 36 000	66 ± 7	12.4 ± 7.7
MDC	3	66 ± 8	30 ± 15	8550 ± 1600	64 ± 7	2.4 ± 3.0
	6	163 ± 38	35 ± 12	24 000 ± 3200	70 ± 4	2.6 ± 0.6
	12	326 ± 64	45 ± 16	59 700 ± 8100	88 ± 12	13.1 ± 4.1
HHMC[a]	3	78 ± 25	60 ± 0	12 200 ± 4100	161 ± 51	18.8 ± 8.1
	6	167 ± 48	55 ± 12	30 200 ± 5800	166 ± 47	20.5 ± 6.6
	12	414 ± 110	70 ± 24	86 300 ± 29 000	145 ± 23	43.9 ± 8.7
HMMC	3	139 ± 56	120 ± 60	32 300 ± 12 000	97 ± 28	8.6 ± 1.6
	6	223 ± 93	90 ± 33	50 500 ± 22 000	98 ± 19	17.1 ± 4.7
	12	390 ± 49	110 ± 24	110 000 ± 12 000	118 ± 19	64.2 ± 9.6

Abbreviations: AUC, area-under-the-curve; C_{last}, last quantifiable concentration; C_{max}, maximum concentration; T_{max}, time of maximum concentration; $t_{1/2}$, elimination half-life.
[a]Results are considered semiquantitative.

HHMC plasma concentrations increased in a dose-related manner. However, it is important to note that plasma concentrations of HHMC reported here must be considered semiquantitative owing to variability when detecting this analyte, as reported in the LC–MS/MS method validation (see Ellefsen *et al*, 2015). C_{max} values for HHMC were 78, 167, and 414 µg/l, while AUC values were 12 200, 30 200, and 86 300 min × µg/l for the 3, 6, and 12 mg/kg methylone doses. HMMC had C_{max} values of 139, 223, and 390 µg/l, and this compound was the primary metabolite as determined by AUC values, which were 32 300, 50 500 and 110 000 min × µg/l. HHMC and HMMC both displayed slower kinetics than methylone and MDC, with HHMC having T_{max} values of 60–70 min and $t_{1/2}$ values of 145–166 min. HMMC had T_{max} values of 90–120 min and $t_{1/2}$ values of 97–118 min.

One of the secondary aims of our PK investigation was to examine the possibility of non-linear accumulation of methylone and its metabolites in the bloodstream. To this end, we compared the expected *vs* observed AUC values for methylone, MDC, HHMC, and HMMC after the 6 and 12 mg/kg doses. To obtain the expected values for each analyte at the 6 and 12 mg/kg doses, the AUC values (mean ± SEM) determined for each analyte at the 3 mg/kg dose were multiplied by a factor of 2 and 4, respectively. Figure 3 demonstrates that observed AUC values for

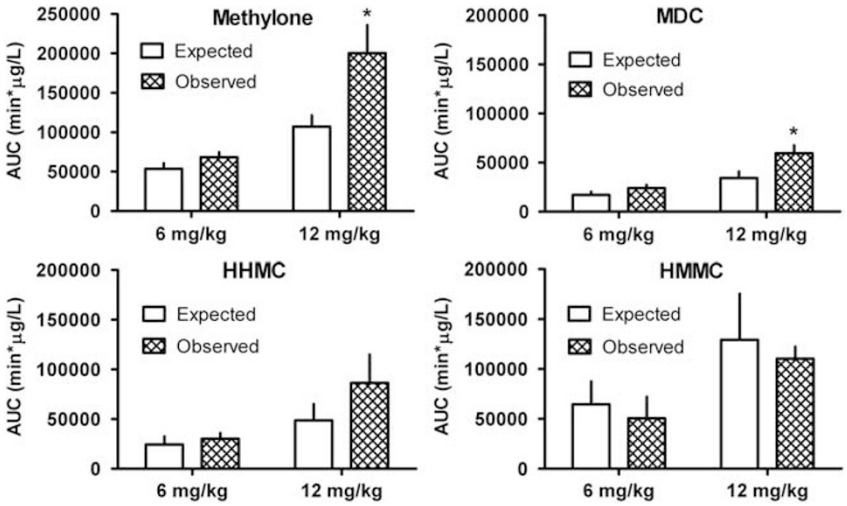

Figure 3 Comparison of expected *vs* observed area-under-the-curve values for methylone, MDC, HHMC, and HMMC. Expected AUCs for each analyte at 6 and 12 mg/kg methylone doses were determined by multiplying the values observed at 3 mg/kg by a factor of 2 and 4, respectively. Data are mean ± SEM for $N = 6/7$ rats per group. $^*p < 0.05$ *vs* expected value at the corresponding dose (Bonferroni's *post hoc* test).

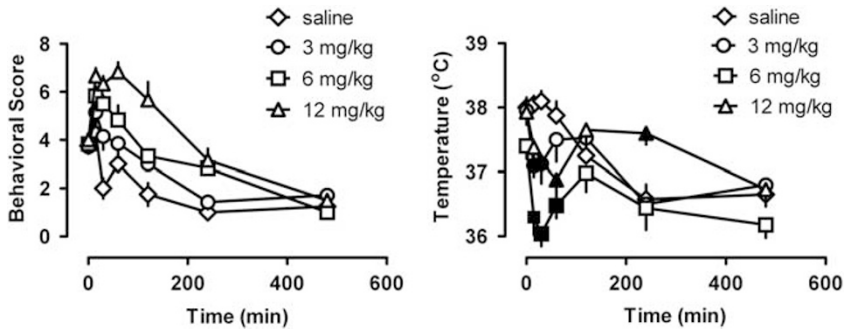

Figure 4 Pharmacodynamic data for rats receiving sc injection of 0 (saline), 3, 6, and 12 mg/kg methylone. Behavioral score and core temperature were determined at 15, 30, 60, 120, 240, and 480 min postinjection as described in Materials and Methods section. Data are mean ± SEM for N = 6/7 rats per group. For temperature data, the filled symbols represent significant effects when compared with saline-injected control rats at corresponding time points ($p < 0.05$, Bonferroni's *post hoc* test).

methylone were greater than expected ($F_{1,20} = 3.95$, $p < 0.01$) but this effect was only significant for the 12 mg/kg dose of drug. Similarly, AUC values for MDC were greater than expected ($F_{1,20} = 2.62$, $p < 0.01$) and this difference reached significance at 12 mg/kg. For HHMC and HMMC, observed AUC values were within the expected range.

Pharmacodynamic Effects of Methylone

Figure 4 depicts the effects of methylone administration on pharmacodynamic end points (ie, locomotor behavior and core body temperature) that correspond to the PK data illustrated in Figure 2. Methylone produced a significant increase in motor activation as revealed by Friedman's test ($p < 0.0021$), and a *post hoc* Dunn's test showed that behavioral score was significantly greater than saline control at the 12 mg/kg dose. Methylone also affected core temperature, with significant main effects of dose ($F_{3,147} = 22.95$, $p < 0.0001$), time ($F_{6,147} = 11.82$, $p < 0.0001$), and dose × time interaction ($F_{18,147} = 2.95$, $p < 0.001$). *Post hoc* tests showed that 3 mg/kg methylone decreased temperature at 15 and 30 min postinjection, whereas 6 mg/kg decreased temperature at 15, 30, and 60 min postinjection. The effects of 12 mg/kg methylone on temperature were biphasic, with decreases at 15, 30, and 60 min followed by increases at 240 min postinjection.

As PK measures and pharmacodynamic data were obtained from the same subjects, we were able to examine correlations between plasma analyte concentrations, behavioral score, and temperature. Table 2 summarizes the Pearson's correlation findings based on evaluation of the mean data depicted in Figures 2 and 4. Overall, behavioral score was positively correlated with plasma concentrations of methylone ($r = 0.771$, $p < 0.001$), MDC ($r = 0.867$, $p < 0.001$), and HHMC ($r = 0.660$, $p < 0.003$) but not HMMC. By contrast, core temperature did not correlate with methylone or any of its metabolites.

Effects of Methylone and its Metabolites *In Vitro*

Our correlation findings suggested that MDC and HHMC might contribute to the behavioral effects of methylone *in vivo*, as suggested by Lopez-Arnau *et al* (2013), so we next examined the ability of methylone and its metabolites to interact with monoamine transporters *in vitro*. Table 3 reports the potency (EC_{50}) and efficacy (% maximal) for each compound to stimulate release of [^{3}H]MPP^+ at DAT and NET and release of [^{3}H]5-HT at SERT. In agreement with our previous findings, methylone acted as a fully efficacious substrate-type releaser at DAT, NET, and SERT, with roughly equal potencies at DAT and NET and slightly lower potency at SERT. MDC was a fully efficacious releaser and showed a selectivity profile similar to methylone. HHMC was a potent efficacious releaser at DAT and NET but weak at SERT. The dihydroxy metabolite was highly selective for the catecholamine transporters, exhibiting a DAT/SERT ratio of 155. In contrast to the other compounds, HMMC was a weak releaser, with potencies $>5\,\mu M$ at all transporter sites.

Effects of Methylone and its Metabolites *In Vivo*

The findings from the *in vitro* transporter assays demonstrated that MDC and HHMC are potent and efficacious releasers. Thus we next utilized *in vivo* microdialysis in rat nucleus accumbens to examine the effects of iv administration of methylone, MDC, HHMC, and HMMC on neurochemistry and behavior. Figure 5 depicts the effects of iv administration of methylone and its metabolites on extracellular dopamine. Methylone produced dose-related elevations in dialysate dopamine ($F_{1,99}=83.81$, $p<0.0001$), with significant increases above saline control at the 1 and 3 mg/kg doses. The maximal rise in dopamine was 2-fold after 1 mg/kg and 3.5-fold after 3 mg/kg. MDC also elevated dopamine ($F_{1,99}=44.60$, $p<0.0001$), but the metabolite had less robust effects when compared with methylone. In contrast to MDC, neither HHMC nor HMMC altered extracellular dopamine concentrations after iv injection.

Figure 6 illustrates the effects of iv administration of methylone and its metabolites on extracellular 5-HT. Methylone produced robust dose-related elevations in dialysate 5-HT ($F_{1,99}=41.85$, $p<0.0001$), with significant increases above saline control at both doses. The magnitude of 5-HT elevations reached 7- and 14-fold above baseline after the 1 and 3 mg/kg methylone doses, respectively. MDC also elevated 5-HT ($F_{1,99}=61.71$, $p<0.0001$), but the metabolite had somewhat smaller effects when compared with methylone, with maximal increases of 4- and 11-fold after the 1 and 3 mg/kg doses. Neither of the hydroxylated metabolites altered extracellular 5-HT concentrations after iv injection. The data in Figure 7 depict the effects of methylone, MDC, HHMC, and HMMC on locomotor activity. Methylone transiently stimulated motor activity ($F_{1,99}=7.77$, $p<0.005$), with significant increases at the first time point after 1 and 3 mg/kg doses. MDC also increased motor activity ($F_{1,99}=7.17$, $p<0.01$), but this effect reached statistical significance only after the 3 mg/kg dose. Neither HHMC nor HMMC affected motor activity after iv injection.

Table 2 Correlations Between Analyte Concentrations and Specific Pharmacodynamic Parameters

Analytes	Parameter	Pearson's *r*	R^2	*p*
Methylone (μg/l)	Behavioral score	0.771	0.595	<0.001
Methylone (μg/l)	Temperature (°C)	0.126	0.016	0.619 (NS)
MDC (μg/l)	Behavioral score	0.867	0.752	<0.001
MDC (μg/l)	Temperature (°C)	0.235	0.055	0.168 (NS)
HHMC (μg/l)	Behavioral score	0.660	0.435	0.003
HHMC (μg/l)	Temperature (°C)	0.281	0.079	0.259 (NS)
HMMC (μg/l)	Behavioral score	0.416	0.173	0.086 (NS)
HMMC (μg/l)	Temperature (°C)	0.456	0.208	0.057 (NS)

Abbreviations: NS, nonsignificant; Pearson's *r*, correlation coefficient; R^2, goodness of fit for linear regression or R squared.

DISCUSSION

Methylone is a popular drug of abuse, yet few studies have addressed its PK and metabolism in animal models (Kamata *et al*, 2006; Lopez-Arnau *et al*, 2013). Here we examined the plasma PK profiles and pharmacodynamic effects for methylone and its phase I metabolites in conscious rats. There are three main findings from the present study. First, methylone is extensively metabolized in a manner similar to its structural analog MDMA, as illustrated by the formation of *O*-demethylenated metabolites (ie, HHMC and HMMC) and an *N*-demethylated metabolite (ie, MDC). In general, plasma concentrations of methylone and its metabolites displayed more rapid kinetics when compared with MDMA (Baumann *et al*, 2009; Concheiro *et al*, 2014). Second, we

Table 3 Effects of Methylone, MDC, HHMC, and HMMC on the Release of [^{3}H]MPP^+ from DAT and NET, and [^{3}H]5-HT From SERT, in Rat Brain Synaptosomes

Test drug	DAT release, EC_{50}, nM ± SD (% max)	NET release, EC_{50}, nM ± SD (% max)	SERT release, EC_{50}, nM ± SD (% max)	DAT/SERT ratio
Methylone	203 ± 31 (100)	164 ± 28 (95)	708 ± 72 (102)	3.5
MDC	370 ± 49 (103)	394 ± 73 (101)	966 ± 145 (97)	2.6
HHMC	90 ± 12 (92)	110 ± 22 (89)	14 100 ± 6700 (75)	155
HMMC	5840 ± 1460 (98)	6340 ± 2540 (100)	7210 ± 2590 (70)	1.2

Data are EC_{50} expressed as nM concentrations (mean ± SD) for $N=3$ experiments performed in triplicate. % Max indicates efficacy compared with saturating concentrations of tyramine as described in Materials and Methods section. DAT/SERT ratio = 1/(DAT EC_{50}) divided by 1/(SERT EC_{50}); higher values reflect greater DAT selectivity.

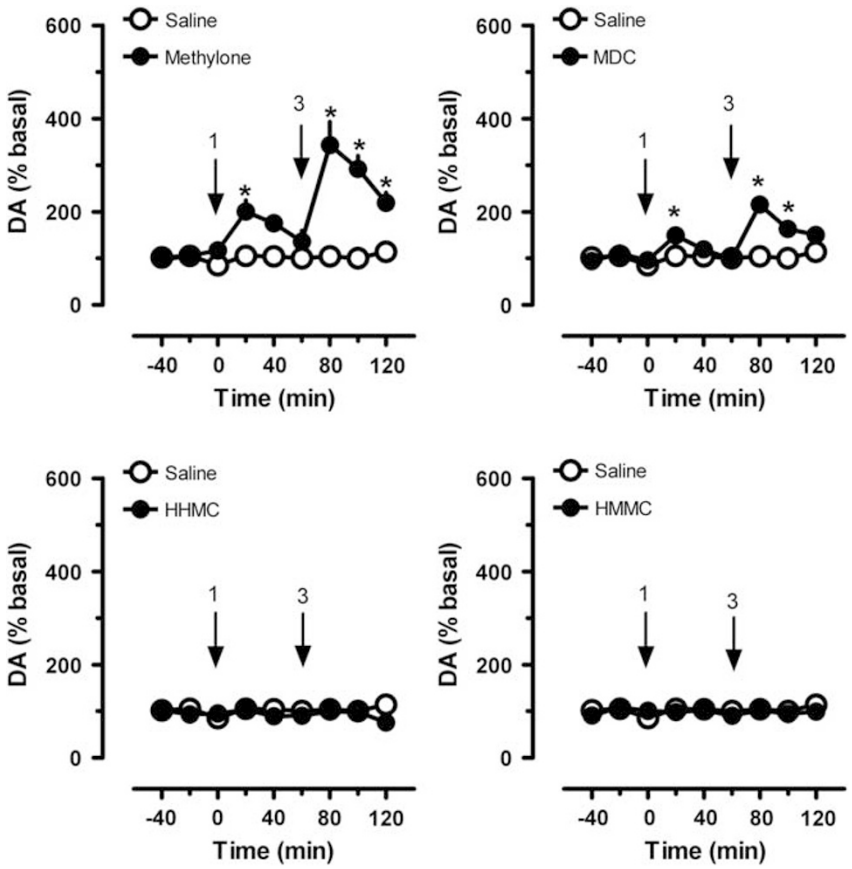

Figure 5 Dose–response effects of methylone, MDC, HHMC, and HMMC on extracellular dopamine (DA) in male rats undergoing *in vivo* microdialysis in nucleus accumbens. Drug-treated rats received iv injections of 1 mg/kg at time 0, followed by 3 mg/kg 60 min later. Control rats received iv saline injections (1 ml/kg) on the same schedule. Data are mean ± SEM for $N = 6/7$ rats per group, expressed as a percentage of preinjection baseline values (% basal). Mean basal dialysate DA concentration for all the treatment groups was 1.55 ± 0.35 pg/5 μl ($N = 34$ rats). *$p < 0.05$ *vs* saline control at the corresponding time point (Bonferroni's *post hoc* test).

present the first *in vivo* evidence for non-linear PK after high-dose methylone administration, which is characterized by increases in circulating concentrations of methylone and MDC that are greater than dose-proportional. Finally, the metabolites MDC and HHMC are potent substrate-type releasers at monoamine transporters as assessed *in vitro*, but only MDC affects brain neurochemistry and locomotor behavior when administered *in vivo*. Taken together, the findings indicate that MDC is the only metabolite that could contribute to the psychoactive effects of systemically administered methylone, but this metabolite is found at much lower concentrations than the parent compound.

One of the primary aims of our study was to examine methylone PKs at sc doses in rats that are relevant to doses abused by humans (eg, 1–3 mg/kg, oral dosing) (see https://www.erowid.org/chemicals/methylone/methylone_dose.shtml for human self-reported dosages). Although dose extrapolations across species are difficult to make because no controlled studies have examined methylone administration in humans, we found methylone C_{max} values of 620, 1410, and 3170 μg/l after sc doses of 3, 6, and 12 mg/kg, respectively. These plasma concentrations from rats fall within the range of values (60–3400 μg/l) detected in human blood specimens reported from case studies, which represent the sole point of comparison between rodent and human data (Barrios *et al*, 2015; Carbone *et al*, 2013; Cawrse *et al*, 2012; Knoy *et al*, 2014; Kovacs *et al*, 2012; McIntyre *et al*, 2013).

Methylone exhibited rapid kinetics compared with its structural analog MDMA, with T_{max} occurring at 15 min as opposed to 36, 54, and 66 min for 2.5, 5, and 10 mg/kg MDMA, respectively (Concheiro *et al*, 2014). Owing to the rapid PKs of methylone after sc administration, it is plausible that T_{max} may have occurred even earlier than 15 min, if specimens had been collected earlier. MDC reached peak concentrations more slowly than methylone and persisted for longer. Plasma concentrations of HHMC reached T_{max} within 1 h, but more quickly than HMMC, which is consistent with the formation of HMMC from the diol metabolite, HHMC (see Figure 1). Importantly, in agreement with the past metabolic analyses of methylone in urine (Kamata *et al*, 2006), HMMC was the predominant metabolite in plasma. The relatively slow formation and clearance of HMMC make it a potential target for toxicological identification of methylone exposure.

It is well established that MDMA displays non-linear PKs in rats and humans (Baumann *et al*, 2009; Chu *et al*, 1996; Concheiro *et al*, 2014; de la Torre *et al*, 2000; Kolbrich *et al*, 2008) owing to inhibition of its own metabolism (Heydari *et al*, 2004; Wu *et al*, 1997). By contrast, Lopez-Arnau *et al* (2013) found no evidence for non-linear PKs in rats after oral

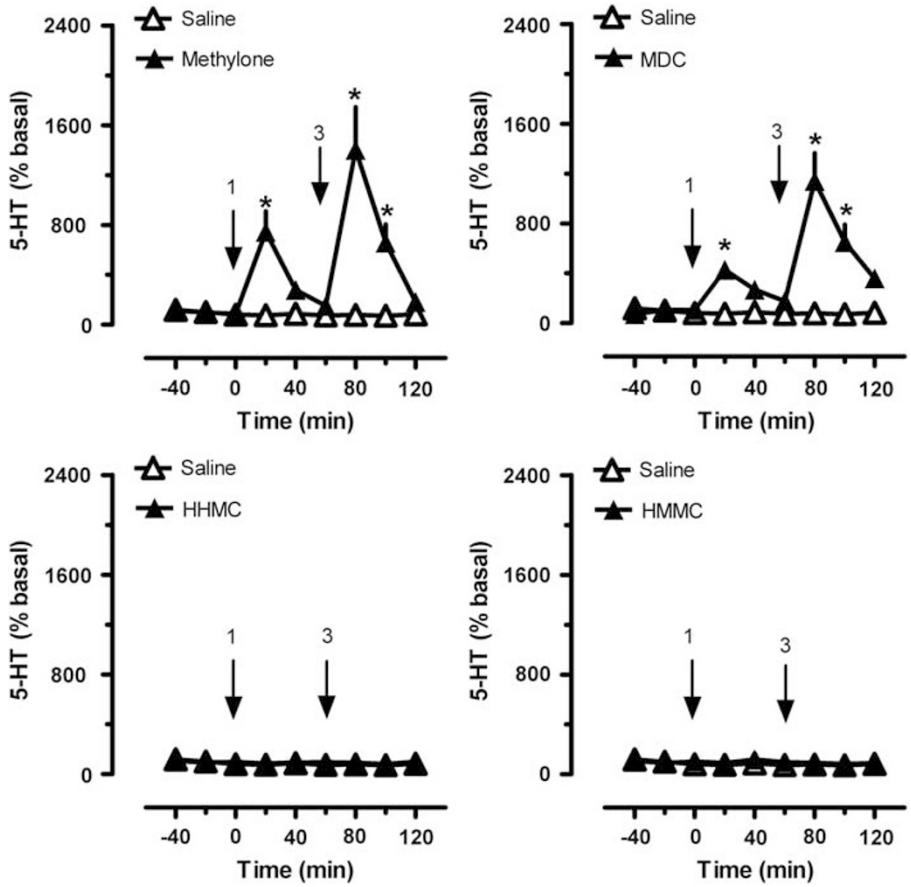

Figure 6 Dose–response effects of methylone, MDC, HHMC, and HMMC on extracellular serotonin (5-HT) in male rats undergoing *in vivo* microdialysis in nucleus accumbens. Drug-treated rats received iv injections of 1 mg/kg at time 0, followed by 3 mg/kg 60 min later. Control rats received iv saline injections (1 ml/kg) on the same schedule. Data are mean ± SEM for $N = 6/7$ rats per group, expressed as a percentage of preinjection baseline values (% basal). Mean basal dialysate 5-HT concentration for all the groups was 0.42 ± 0.11 pg/5 µl ($N = 34$ rats). *$p < 0.05$ *vs* saline control at the corresponding time point (Bonferroni's *post hoc* test).

administration of methylone at 15 and 30 mg/kg. For linear kinetics to be observed in the present study, an increase in dose from 3 to 6 mg/kg should produce a doubling of AUC values for methylone and its metabolites, while an increase from 3 to 12 mg/kg should produce a 4-fold increase in AUC values. The data in Figure 3 clearly demonstrate that plasma concentrations of methylone and MDC increase more than expected based on the doses administered, providing an indication of non-linear accumulation for these analytes in plasma. Methylone inhibits human CYP2D6 *in vitro* (Dinger *et al*, 2016; Pedersen *et al*, 2013), and the present non-linear increases in plasma methylone and MDC seem to agree with this observation. It should be mentioned that non-linear kinetics resulting from inhibition of CYP2D1 (ie, the rat isoform of CYP2D6 responsible for methylone *O*-demethylenation) should result in appreciable decreases in the formation of HHMC and HMMC (see Concheiro *et al*, 2014). However, Figure 3 illustrates that AUC values for HHMC and HMMC were within the expected range as dose increased, not less than predicted. Thus additional research utilizing a broader range of methylone doses will be needed to definitely demonstrate the phenomenon of non-linear PK for methylone.

Our PK study employed rats bearing indwelling iv catheters, which allowed repeated stress-free blood sampling, along with measurement of locomotor behavior and core temperature by non-invasive methods. The behavioral activity scoring system used for our experiments is sensitive to dose-dependent changes in locomotor activation produced by psychomotor stimulants, such as cocaine (Baumann *et al*, 1993; Kalivas *et al*, 1988). Specifically, as the dose of drug is increased, the predominant behaviors change from exploratory ambulation and rearing to repetitive stereotypic movements. We found that methylone produced dose-related increases in motor activity with concomitant decreases in temperature. Methylone-induced locomotor activation was positively correlated with plasma concentrations of methylone, MDC, and HHMC, whereas core temperature failed to correlate with any analyte measured (see Table 2). Overall, the PK and pharmacodynamic results suggested that MDC and HHMC might contribute significantly to behavioral effects, but not temperature changes, produced by systemically administered methylone.

It is now well established that methylone acts as a substrate-type releaser at DAT, NET, and SERT in rat brain tissue and in cells expressing human transporters (Baumann *et al*, 2012; Eshleman *et al*, 2013; Simmler *et al*, 2013). Thus

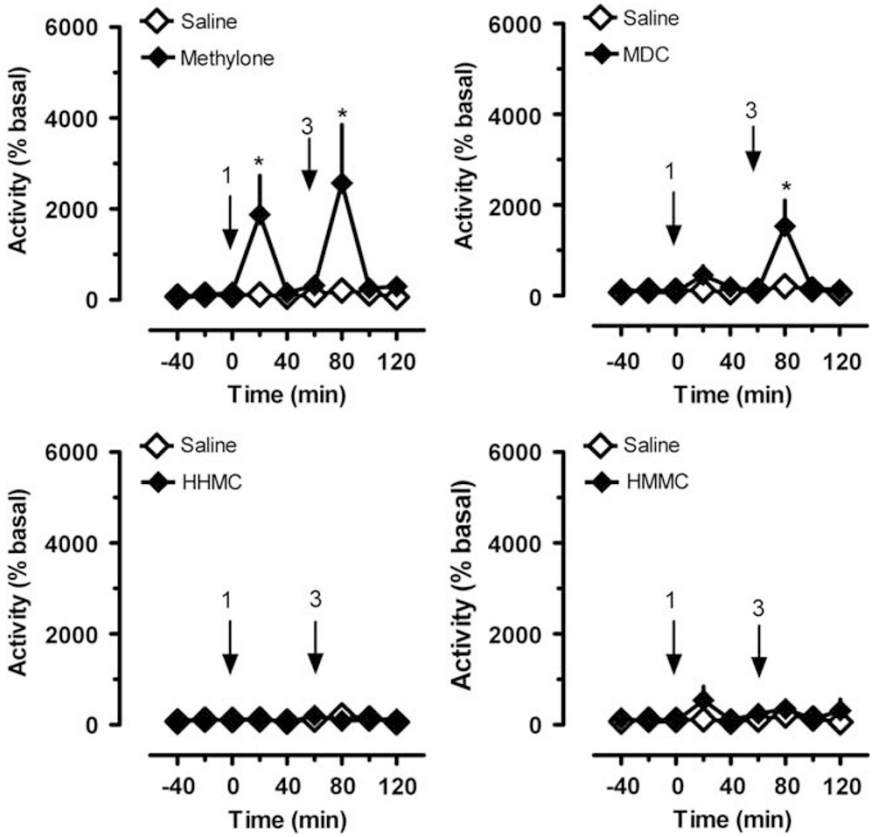

Figure 7 Dose–response effects of methylone, MDC, HHMC, and HMMC on forward locomotion (activity) in male rats undergoing *in vivo* microdialysis in nucleus accumbens. Drug-treated rats received iv injections of 1 mg/kg at time 0, followed by 3 mg/kg 60 min later. Control rats received iv saline injections (1 ml/kg) on the same schedule. Data are mean ± SEM for $N = 6/7$ rats per group, expressed as a percentage of preinjection baseline values (% basal). Mean basal activity was 86 ± 22 cm/20 min bin (N = 34 rats). *$p < 0.05$ *vs* saline control at the corresponding time point (Bonferroni's *post hoc* test).

we wished to examine the effects of methylone metabolites using *in vitro* transporter release assays in rat brain synaptosomes. In agreement with previous findings, methylone acted as a potent and efficacious releaser, with slightly higher potency at DAT and NET as compared with SERT (Baumann *et al*, 2012). MDC had a similar release profile but was weaker at all three transporters. The data reported here for MDC differ somewhat from findings with 3,4-methylenedioxyamphetamine (MDA), the analogous *N*-demethylated metabolite of MDMA. We and others have shown that MDA and MDMA display nearly identical potency and selectivity as substrate-type releasers at monoamine transporters *in vitro* (McKenna *et al*, 1991; Sandtner *et al*, 2016; Wichems *et al*, 1995). Interestingly, HHMC was found to be a potent and selective substrate for DAT and NET, with a DAT/SERT ratio of 155 *in vitro*. In fact, HHMC was more potent than methylone as a releaser at DAT and NET. By contrast, HMMC was very weak at all transporters.

Because we found that MDC and HHMC were potent efficacious releasers at monoamine transporters, we sought to examine the neurochemical and behavioral effects of these metabolites when administered *in vivo*. Consistent with previous work (Baumann *et al*, 2012; Schindler *et al*, 2016), we found that methylone produced dose-related elevations in extracellular dopamine and 5-HT in rat nucleus accumbens, with larger effects on extracellular 5-HT. Importantly, the iv doses of methylone tested here in microdialysis experiments are in the range of those self-administered by rats (Schindler *et al*, 2016; Vandewater *et al*, 2015; Watterson *et al*, 2012). Administration of MDC increased dopamine and 5-HT as well, but weakly compared with methylone. The microdialysis data with MDC are generally consistent with its lower potency at DAT and SERT but differ from results obtained with MDA (Baumann *et al*, 2007; Kankaanpaa *et al*, 1998; Nash and Nichols, 1991). For example, Kankaanpaa *et al* (1998) showed that MDA administration to rats induced elevations in extracellular dopamine and 5-HT in the nucleus accumbens that were greater than those produced by MDMA. Dal Cason *et al* (1997) examined the discriminative stimulus properties of MDC and reported the compound fully substitutes for the stimulus cue in MDMA-trained rats but not in amphetamine-trained rats, consistent with the notion that MDC has somewhat greater effects on 5-HT systems *in vivo* as compared with dopamine systems (Dal Cason *et al*, 1997).

Surprisingly, we found that neither HHMC nor HMMC altered dialysate neurotransmitter concentrations after iv administration at the doses tested. Examination of the locomotor behavior during microdialysis sampling demonstrated that methylone and MDC stimulated activity but HHMC and HMMC did not. When combined with the *in vitro* results, the microdialysis data suggest that HHMC

may not cross the blood–brain barrier, perhaps owing to its increased polarity relative to methylone. Indeed, the total polar surface area for HHMC is 69.55 as compared with 47.57 for methylone (http://www.molinspiration.com/cgi-bin/properties). It seems feasible that administration of higher doses of HHMC might produce centrally mediated effects, but this possibility requires further study. Additionally, as CYP enzymes are present in brain tissue, HHMC could be produced locally in the brain after systemic administration of methylone. In previous studies, we found that 3,4-dihydroxymethamphetamine, the *O*-demethylenated metabolite of MDMA, does not appear to penetrate into the brain but has powerful cardiovascular effects *in vivo* (Schindler *et al*, 2014). Thus further studies are needed to examine the possible cardiovascular effects of HHMC, based on its potent releasing activity at NET.

In conclusion, we report the first plasma PK profiles for methylone and its metabolites in conscious freely moving rats and provide evidence for non-linear accumulation of methylone and MDC after high-dose administration. The metabolites MDC and HHMC are potent efficacious substrate-type releasers at monoamine transporters as assessed *in vitro*, but only MDC produces centrally mediated neurochemical and behavioral changes when administered *in vivo*. HMMC is the most predominant and persistent metabolite of methylone, making HMMC a good target for forensic drug testing to confirm methylone exposure, expanding the window of detection. Further studies are necessary to more fully explore the phenomenon of non-linear PKs and its associated pharmacodynamic consequences after high-dose methylone administration.

FUNDING AND DISCLOSURE

This research was generously supported by the Intramural Research Program of the National Institute on Drug Abuse, National Institutes of Health. The authors declare no conflicts of interest.

REFERENCES

Barrios L, Grison-Hernando H, Boels D, Bouquie R, Monteil-Ganiere C, Clement R (2015). Death following ingestion of methylone. *Int J Legal Med* **130**: 381–385.

Baumann MH, Ayestas MA Jr., Partilla JS, Sink JR, Shulgin AT, Daley PF *et al* (2012). The designer methcathinone analogs, mephedrone and methylone, are substrates for monoamine transporters in brain tissue. *Neuropsychopharmacology* **37**: 1192–1203.

Baumann MH, Partilla JS, Lehner KR (2013). Psychoactive 'bath salts': not so soothing. *Eur J Pharmacol* **698**: 1–5.

Baumann MH, Raley TJ, Partilla JS, Rothman RB (1993). Biosynthesis of dopamine and serotonin in the rat brain after repeated cocaine injections: a microdissection mapping study. *Synapse* **14**: 40–50.

Baumann MH, Wang X, Rothman RB (2007). 3,4-Methylenedioxymethamphetamine (MDMA) neurotoxicity in rats: a reappraisal of past and present findings. *Psychopharmacology* **189**: 407–424.

Baumann MH, Zolkowska D, Kim I, Scheidweiler KB, Rothman RB, Huestis MA (2009). Effects of dose and route of administration on pharmacokinetics of (+ or -)-3,4-methylenedioxymethamphetamine in the rat. *Drug Metab Dispos* **37**: 2163–2170.

Carbone PN, Carbone DL, Carstairs SD, Luzi SA (2013). Sudden cardiac death associated with methylone use. *Am J Forensic Med Pathol* **34**: 26–28.

Cawrse BM, Levine B, Jufer RA, Fowler DR, Vorce SP, Dickson AJ *et al* (2012). Distribution of methylone in four postmortem cases. *J Anal Toxicol* **36**: 434–439.

Chu T, Kumagai Y, DiStefano EW, Cho AK (1996). Disposition of methylenedioxymethamphetamine and three metabolites in the brains of different rat strains and their possible roles in acute serotonin depletion. *Biochem Pharmacol* **51**: 789–796.

Concheiro M, Baumann MH, Scheidweiler KB, Rothman RB, Marrone GF, Huestis MA (2014). Nonlinear pharmacokinetics of (+/-)3,4-methylenedioxymethamphetamine (MDMA) and its pharmacodynamic consequences in the rat. *Drug Metab Dispos* **42**: 119–125.

Dal Cason TA, Young R, Glennon RA (1997). Cathinone: an investigation of several N-alkyl and methylenedioxy-substituted analogs. *Pharmacol Biochem Behav* **58**: 1109–1116.

de la Torre R, Farre M (2004). Neurotoxicity of MDMA (ecstasy): the limitations of scaling from animals to humans. *Trends Pharmacol Sci* **25**: 505–508.

de la Torre R, Farre M, Ortuno J, Mas M, Brenneisen R, Roset PN *et al* (2000). Non-linear pharmacokinetics of MDMA ('ecstasy') in humans. *Br J Clin Pharmacol* **49**: 104–109.

Dinger J, Meyer MR, Maurer HH (2016). *In vitro* cytochrome P450 inhibition potential of methylenedioxy-derived designer drugs studied with a two-cocktail approach. *Arch Toxicol* **90**: 305–318.

Drug Enforcement Administration DoJ (2011). Schedules of controlled substances: temporary placement of three synthetic cathinones in Schedule I. Final Order. *Fed Regist* **76**: 65371–65375.

Drug Enforcement Administration DoJ (2013). Establishment of drug codes for 26 substances. Final rule. *Fed Regist* **78**: 664–666.

Ellefsen K, Concheiro M, Suzuki M, Rice K, Elmore J, Baumann M *et al* (2015). Quantification of methylone and metabolites in rat and human plasma by liquid chromatography-tandem mass spectrometry. *Forensic Toxicol* **33**: 202–212.

Eshleman AJ, Wolfrum KM, Hatfield MG, Johnson RA, Murphy KV, Janowsky A (2013). Substituted methcathinones differ in transporter and receptor interactions. *Biochem Pharmacol* **85**: 1803–1815.

Glennon RA (2014). Bath salts, mephedrone, and methylenedioxypyrovalerone as emerging illicit drugs that will need targeted therapeutic intervention. *Adv Pharmacol* **69**: 581–620.

Grecco GG, Sprague JE (2016). Impact of functional group modifications on designer phenethylamine induced hyperthermia. *Chem Res Toxicol* **29**: 871–878.

Heydari A, Yeo KR, Lennard MS, Ellis SW, Tucker GT, Rostami-Hodjegan A (2004). Mechanism-based inactivation of CYP2D6 by methylenedioxymethamphetamine. *Drug Metab Dispos* **32**: 1213–1217.

Kalivas PW, Duffy P, DuMars LA, Skinner C (1988). Behavioral and neurochemical effects of acute and daily cocaine administration in rats. *J Pharmacol Exp Ther* **245**: 485–492.

Kamata HT, Shima N, Zaitsu K, Kamata T, Miki A, Nishikawa M *et al* (2006). Metabolism of the recently encountered designer drug, methylone, in humans and rats. *Xenobiotica* **36**: 709–723.

Kankaanpaa A, Meririnne E, Lillsunde P, Seppala T (1998). The acute effects of amphetamine derivatives on extracellular serotonin and dopamine levels in rat nucleus accumbens. *Pharmacol Biochem Behav* **59**: 1003–1009.

Kiyatkin EA, Kim AH, Wakabayashi KT, Baumann MH, Shaham Y (2015). Effects of social interaction and warm ambient temperature on brain hyperthermia induced by the designer drugs methylone and MDPV. *Neuropsychopharmacology* **40**: 436–445.

Knoy JL, Peterson BL, Couper FJ (2014). Suspected impaired driving case involving alpha-pyrrolidinovalerophenone, methylone and ethylone. *J Anal Toxicol* **38**: 615–617.

Kolbrich EA, Goodwin RS, Gorelick DA, Hayes RJ, Stein EA, Huestis MA (2008). Plasma pharmacokinetics of 3,4-methylenedioxymethamphetamine after controlled oral administration to young adults. *Ther Drug Monit* **30**: 320–332.

Kovacs K, Toth AR, Kereszty EM (2012). [A new designer drug: methylone related death]. *Orvosi Hetilap* **153**: 271–276.

Lopez-Arnau R, Martinez-Clemente J, Carbo M, Pubill D, Escubedo E, Camarasa J (2013). An integrated pharmacokinetic and pharmacodynamic study of a new drug of abuse, methylone, a synthetic cathinone sold as 'bath salts'. *Prog Neuropsychopharmacol Biol Psychiatry* **45**: 64–72.

Lopez-Arnau R, Martinez-Clemente J, Pubill D, Escubedo E, Camarasa J (2014). Serotonergic impairment and memory deficits in adolescent rats after binge exposure of methylone. *J Psychopharmacol* **28**: 1053–1063.

McIntyre IM, Hamm CE, Aldridge L, Nelson CL (2013). Acute methylone intoxication in an accidental drowning–a case report. *Forensic Sci Int* **231**: e1–e3.

McKenna DJ, Guan XM, Shulgin AT (1991). 3,4-Methylenedioxyamphetamine (MDA) analogues exhibit differential effects on synaptosomal release of 3H-dopamine and 3H-5-hydroxytryptamine. *Pharmacol Biochem Behav* **38**: 505–512.

Nash JF, Nichols DE (1991). Microdialysis studies on 3,4-methylenedioxyamphetamine and structurally related analogues. *Eur J Pharmacol* **200**: 53–58.

Pedersen AJ, Petersen TH, Linnet K (2013). In vitro metabolism and pharmacokinetic studies on methylone. *Drug Metab Dispos* **41**: 1247–1255.

Ridpath A, Driver CR, Nolan ML, Karpati A, Kass D, Paone D *et al* (2014). Illnesses and deaths among persons attending an electronic dance-music festival - New York City, 2013. *MMWR Morb Mortal Wkly Rep* **63**: 1195–1198.

Rothman RB, Baumann MH, Dersch CM, Romero DV, Rice KC, Carroll FI *et al* (2001). Amphetamine-type central nervous system stimulants release norepinephrine more potently than they release dopamine and serotonin. *Synapse* **39**: 32–41.

Sandtner W, Stockner T, Hasenhuetl PS, Partilla JS, Seddik A, Zhang YW *et al* (2016). Binding mode selection determines the action of ecstasy homologs at monoamine transporters. *Mol Pharmacol* **89**: 165–175.

Schindler CW, Thorndike EB, Blough BE, Tella SR, Goldberg SR, Baumann MH (2014). Effects of 3,4-methylenedioxymethamphetamine (MDMA) and its main metabolites on cardiovascular function in conscious rats. *Br J Pharmacol* **171**: 83–91.

Schindler CW, Thorndike EB, Goldberg SR, Lehner KR, Cozzi NV, Brandt SD *et al* (2016). Reinforcing and neurochemical effects of the 'bath salts' constituents 3,4-methylenedioxypyrovalerone (MDPV) and 3,4-methylenedioxy-N-methylcathinone (methylone) in male rats. *Psychopharmacology* **233**: 1981–1990.

Simmler LD, Buser TA, Donzelli M, Schramm Y, Dieu LH, Huwyler J *et al* (2013). Pharmacological characterization of designer cathinones in vitro. *Br J Pharmacol* **168**: 458–470.

Vandewater SA, Creehan KM, Taffe MA (2015). Intravenous self-administration of entactogen-class stimulants in male rats. *Neuropharmacology* **99**: 538–545.

Warrick BJ, Wilson J, Hedge M, Freeman S, Leonard K, Aaron C (2012). Lethal serotonin syndrome after methylone and butylone ingestion. *J Med Toxicol* **8**: 65–68.

Watterson LR, Hood L, Sewalia K, Tomek SE, Yahn S, Johnson CT *et al* (2012). The reinforcing and rewarding effects of methylone, a synthetic cathinone commonly found in 'bath salts'. *J Addict Res Ther* **Suppl 9**: pii 002.

Wichems CH, Hollingsworth CK, Bennett BA (1995). Release of serotonin induced by 3,4-methylenedioxymethamphetamine (MDMA) and other substituted amphetamines in cultured fetal raphe neurons: further evidence for calcium-independent mechanisms of release. *Brain Res* **695**: 10–18.

Wu D, Otton SV, Inaba T, Kalow W, Sellers EM (1997). Interactions of amphetamine analogs with human liver CYP2D6. *Biochem Pharmacol* **53**: 1605–1612.